

# CFM: SIMT Thread Divergence Reduction by Melding Similar Control-Flow Regions in GPGPU Programs

Charitha Saumya, Kirshanthan Sundararajah and Milind Kulkarni  
*School of Electrical and Computer Engineering*  
*Purdue University*  
West Lafayette, IN, USA  
cgusthin@purdue.edu, ksundar@purdue.edu, milind@purdue.edu

**Abstract**—GPGPUs use the Single-Instruction-Multiple-Thread (SIMT) execution model where a group of threads—wavefront or warp—execute instructions in lockstep. When threads in a group encounter a branching instruction, not all threads in the group take the same path, a phenomenon known as control-flow divergence. The control-flow divergence causes performance degradation because both paths of the branch must be executed one after the other. Prior research has primarily addressed this issue through architectural modifications. We observe that certain GPGPU kernels with control-flow divergence have similar control-flow structures with similar instructions on both sides of a branch. This structure can be exploited to reduce control-flow divergence by melding the two sides of the branch allowing threads to reconverge early, reducing divergence. In this work, we present CFM, a compiler analysis and transformation framework that can meld divergent control-flow structures with similar instruction sequences. We show that CFM can reduce the performance degradation from control-flow divergence.

## I. INTRODUCTION

General Purpose Graphics Processing Units (GPGPU) are capable of executing thousands of threads in parallel, efficiently. Advancements in the programming models and compilers for GPUs have made it much easier to write data-parallel applications and execute them in GPGPUs. Even though it is straight forward to implement these data-parallel applications, it does not immediately translate to better performance. One key reason for the lack of performance portability is that GPGPUs are not capable of executing all the threads independently. Instead threads are grouped together into units called *warps*, and threads in a warp execute instructions in lockstep. This is commonly referred to as the Single Instruction Multiple Thread (SIMT) execution model.

The SIMT model suffers performance degradation when threads exhibit *irregularity* and can no longer execute in lockstep. Irregularity comes in two forms, irregularity in memory accesses pattern (*i.e.* memory divergence) and irregularity in control-flow of the program (*i.e.* control-flow divergence). Memory divergence occurs when GPGPU threads need to access memory at non-uniform locations, which results in un-coalesced memory accesses. Un-coalesced memory accesses

are bad for GPU performance because memory bandwidth can not be fully utilized to do useful work.

Control-flow divergence occurs when threads in a warp diverge at branch instructions. At the *diverging* branches lockstep execution can not be maintained because threads in a warp may want to execute different basic blocks (*i.e.* diverge). When threads in a warp want to take different control flow paths, they can no longer execute in lockstep. Instead, when executing instructions along a diverged path, GPGPUs mask out the threads that do not want to take that path. The threads *reconverge* at the immediate post-dominator (IPDOM) of a divergent branch—the instruction that all threads from both branches want to execute. This style of IPDOM-based reconvergence is implemented in hardware in most GPGPU architectures to maintain SIMT execution.

Even though IPDOM based reconvergence can handle arbitrary control-flow, it imposes a significant performance penalty if the program has a lot of divergent branches. In the IPDOM reconvergence model, instructions executed on divergent branches necessarily cannot utilize the full width of a SIMD unit. If the code has a lot of nested divergent branches or divergent branches inside loops, this style of execution causes significant under-utilization of SIMD resources. For some GPGPU applications divergent branches are unavoidable, and there have been many techniques proposed to address this issue both in hardware and software.

Proposals such as Dynamic warp formation [1], Thread block compaction [2] and Dual-path execution model [3] focus on mitigating the problem at hardware level by changing how the threads are scheduled for execution and making sure that the threads executing the same instruction are grouped together. Unfortunately, such approaches are not useful on commodity GPGPUs.

There has also been efforts to reduce divergence through compiler approaches that leverage the observation that different control-flow paths often contain similar instruction (sub)sequences. *Tail merging* [4] identifies branches that have identical sequences of code and introduces early jumps to *merged* basic blocks, with the effect of reducing divergence.

TABLE I: Comparison of techniques for control-flow divergence reduction

Control-flow and instruction Pattern	Technique		
	Tail Merging	Branch Fusion	CFM
Diamond control-flow with identical instruction sequences	✓	✓	✓
Diamond control-flow with distinct instruction sequences	✗	✓	✓
Complex control-flow	✗	✗	✓

*Branch fusion* generalizes tail merging to work with instruction sequences that may not be identical [5]. However, it cannot analyze complex control flow and hence is restricted to simple if-then-else branches where if and then consists of a single basic block (*i.e.* diamond shaped control-flow).

This paper introduces a more general software-only approach to exploiting similarity in divergent paths, called *control flow melding*. Control flow melding is a general control-flow transformation which can meld similar control-flow *subgraphs* inside a if-then-else region (not just individual basic blocks). By working hierarchically, recursively merging divergent control flow at the level of subgraphs of the CFG, control flow melding can handle substantially more general control structures than prior work. This paper describes CFM, a realization of control flow melding for general GPGPU programs. Table I compares the capabilities of CFM with branch fusion and tail merging.

CFM works in several steps. First, it detects divergent if-then-else regions and splits the divergent regions into Single Entry Single Exit (SESE) control-flow subgraphs. Next it uses a hierarchical sequence alignment technique to *meld* profitable control-flow subgraphs, repeatedly finding subgraphs whose control flow structures and constituent instructions can be aligned. Once a fixpoint is reached, CFM uses this hierarchical alignment to generate code for the region with reduced control-flow divergence.

The main contributions of the paper are,

- **Control-Flow-Melder (CFM)**, a realization of control flow melding that identifies profitable melding opportunities in divergent if-then-else regions of the control-flow using a hierarchical sequence alignment approach and then transforms the code to meld these regions of the control-flow in to reduce control-flow divergence.
- An implementation of CFM in LLVM [6] that can be applied to GPGPU programs written in HIP [7] or CUDA [8]
- An evaluation of CFM on a set of synthetic GPU programs and a set of real-world GPU applications showing its effectiveness

## II. BACKGROUND

### A. GPUGPU Architecture

Modern GPGPUs have multiple processing cores, each of which contains multiple parallel lanes (*i.e.* SIMD units), a vector register file and a chunk of shared memory. The unit of execution is called a warp (or wavefront). A warp is a

collection of threads executed in lock-step on a SIMD unit. Shared memory is shared among the warps executing on a core. A branch unit takes care of control-flow divergence by maintaining a SIMT stack to enforce IPDOM based reconvergence, as discussed in Section I. GPGPU programming abstractions like CUDA [8] or HIP [7] gives the illusion of data parallelism with independent threads. However, during real execution, a group of program instances (*i.e.* threads) are mapped to a warp and executed in lock-step. Therefore control-flow divergence in SPMD programs is detrimental to the performance because of the SIMT execution limitations.

### B. LLVM SSA form and GPU Divergence Analysis

LLVM [6] is a general framework for building compilers, optimizations and code generators. Most of the widely adopted GPGPU compilers [9], [10] are built on top of the LLVM infrastructure. LLVM uses a target-independent intermediate representation, LLVM-IR, that enables implementing portable compiler optimizations. LLVM-IR uses static single assignment form [11] which requires that every program variable is assigned once and is defined before being used. SSA form uses  $\phi$  nodes to resolve data-flow when branches are present in the control-flow graph, selecting which definition should be chosen at a confluence of different control paths. In GPGPU compilers, a key step in identifying divergent control-flow regions is performing compiler analyses to identify divergent variables (or branches) [5], [12]. A branch is divergent if the branching condition evaluates to a non-uniform value for different threads in a warp. If the branching condition is divergent, threads in a warp will have to take different control-flow paths at this point. LLVM’s divergence analysis tags a branch as divergent, if the branching condition is either data-dependent or sync-dependent on a divergent variable (such as thread ID) [12], though more sophisticated divergence analyses have been proposed [13].

## III. OVERVIEW

Bitonic sort is a parallel sorting algorithm used in many parallel sorting algorithms such as bitonic mergesort and Cederman’s quicksort [14], [15]. Figure 1 shows a CUDA implementation of bitonic sort. This kernel is our running example for describing CFM’s control-flow melding algorithm.

In this kernel, the branch condition at line 8 depends on the *thread ID*. Therefore it is divergent. Since the divergent branch is located inside a loop, the execution of the two sides of the branch needs to be serialized many times, resulting in high control-flow divergence. However the code inside the *if* (line 9-10) and *else* (line 13-14) sections of the divergent branch are similar in two ways. First, both code sections have the same control-flow structure (*i.e.* *if-then* branch). Second, instructions along the two paths are also similar. Both conditions compare two elements in the *shared* array and perform a *swap* operation. Therefore the contents of the *if* and *else* sections can be melded to reduce control-flow divergence. Both codes sections consists of shared memory loads and store operations. In the unmelded version of the code these shared

```

1  __global__ static void bitonicSort(int *values) {
2  // copy data from global memory to shared memory
3  __syncthreads();
4  for (unsigned int k = 2; k <= NUM; k *= 2) {
5      for (unsigned int j = k / 2; j > 0; j /= 2) {
6          unsigned int ixj = tid ^ j;
7          if (ixj > tid) {
8              if ((tid & k) == 0) {
9                  if (shared[ixj] < shared[tid])
10                 swap(shared[tid], shared[ixj]);
11             }
12             else {
13                 if (shared[ixj] > shared[tid])
14                 swap(shared[tid], shared[ixj]);
15             }
16         }
17     }
18     __syncthreads();
19 } // write data back to global memory
20 }

```

Fig. 1: Bitonic sort kernel

memory operations will have to be serialized due to thread-divergence. However, if the two sections are melded threads can issue the memory instructions in the same cycle resulting in improved performance.

Existing compiler optimizations such as tail merging and branch fusion cannot be applied to this case. Tail merging is applicable only if two basic blocks have a common destination and have identical instruction sequences at their tails. However in bitonic sort, the *if* and *then* sections of the divergent branch have multiple basic blocks, and the compiler cannot apply tail merging. Similarly branch fusion requires diamond shaped control-flow and does not work if the *if* and *else* section of the branch contains complex control-flow structures.

CFM solves this problem in two phases. In the analysis phase (Section IV-C), CFM analyzes the control-flow region dominated by a divergent branch to find isomorphic sub-regions that are in the true and false path of the divergent branch. These isomorphic sub-region pairs are aligned based on their melding profitability using a sequence alignment strategy. Melding profitability is a metric computed at compile time to approximate the percentage of thread cycles that can be saved by fusing two control-flow regions. Next, CFM takes the most profitable sub region pair in the alignment and computes a profitable instruction alignment for corresponding basic blocks in the two regions. In the code generation phase (Section IV-D), CFM uses this instruction alignment to meld corresponding basic blocks in the sub-region pair. This melding is applied iteratively until no further profitable melding can be performed. CFM’s melding transformation is done in SSA form, therefore the resulting CFG can be optimized further using other compiler optimizations (Sections IV-E and IV-F).

#### IV. DETAILED DESIGN

In this section we describe the algorithm used by CFM to meld similar control-flow subgraphs.

##### A. Preliminaries and Definitions

First we define the following terms used in our algorithm description.

**Definition 1. Simple Region :** A simple region is a subgraph of a program’s CFG that is connected to the remaining CFG with only two edges, an entry edge and an exit edge.

**Definition 2. Region :** A region of the CFG is characterized by two basic blocks, its entry and exit. Any program path that goes through the region must pass through entry first and exit last. All the basic blocks inside a region are dominated by its entry and post-dominated by its exit. Region with entry  $E$  and exit  $X$  is denoted by the tuple  $(E, X)$ . LLVM regions are defined similarly [16].

**Definition 3. Single Entry Single Exit Subgraph :** Single entry single exit (SESE) subgraph is either a simple region or a single basic block with a single predecessor and a successor.

Note that a region with entry  $E$  and exit  $X$  can be transformed into a simple region by introducing a new entry and exit blocks  $E_{new}$ ,  $X_{new}$ . All successors of  $E$  are moved to  $E_{new}$  and  $E_{new}$  is made the single successor of  $E$ . Similarly, all predecessors of  $X$  are moved to  $X_{new}$  and a single exit edge is added from  $X_{new}$  to  $X$ . Also regions can have subregions within them forming a tree structure called *program structure tree* [17].

**Definition 4. Simplified Region :** A region with all its sub-regions transformed into simple regions is called a simplified region.

We now turn to the steps the CFM compiler pass takes to reduce control divergent code.

##### B. Detecting meldable Divergent Regions

First CFM needs to detect divergent branches in the CFG. We use LLVM’s built-in divergence analysis to decide if a branch is divergent or not (Section II). The smallest CFG region enclosing a divergent branch is called the *divergent region* corresponding to this branch.

Melding transformation is applied only to divergent regions of the CFG. The next step is to decide if a divergent region contains control-flow subgraphs (definition 3) that can be safely melded.

**Definition 5. Meldable Divergent Region:** A simplified region  $R$  with entry  $E$  and exit  $X$  is said to be meldable and divergent if the following conditions are met,

- 1) The entry block of  $R$  has a divergent branch
- 2) Let  $B_T$  and  $B_F$  be the successor blocks of  $E$ .  $B_T$  does not post-dominate  $B_F$  and  $B_F$  does not post-dominate  $B_T$

According to definition 5, a *meldable divergent region* has a divergent branch at its entry (condition 1). This makes sure that our melding transformation is only applied to divergent regions, and non-divergent parts of the control-flow are left untouched. Condition 2 ensures that paths  $B_T \rightarrow X$  (*i.e.* true

path) and  $B_F \rightarrow X$  (i.e. false path) consists of at least one SESE subgraph and these subgraphs from the two paths can potentially be melded to reduce control-flow divergence.

**Example :** Consider our running example in Figure 1. When this kernel is compiled with *ROCm HIPCC* GPU compiler [7] with *-O3* optimization level into LLVM-IR, we get the CFG shown in Figure 5a. Note that the compiler aggressively unrolls both the loops (lines 4 and 5) in the kernel, and the resulting CFG consists of multiple repeated segments of the inner loop’s body (lines 6-17). In Figure 5a, only one unrolled instantiation of the loop body is shown. As explained in Section III, this kernel contains a divergent branch, which is at the end of basic block  $\%B$ . Also  $\%B$ ’s two successors  $\%C$  and  $\%D$  do not post-dominate each other. Therefore the region  $(\%B, \%G)$  is a meldable divergent region.

### C. Computing Melding Profitability

Definition 5 only allows us to detect regions that contain meldable control-flow subgraphs. It does not tell us whether melding them will improve performance. In order to check the profitability of melding we employ a hierarchical sequence alignment method. First, we compute an optimal alignment of SESE subgraphs within a meldable divergent region, and second we compute optimal instruction alignments for instructions within the aligned SESE subgraphs. If this hierarchical alignment is proved to be profitable relative to the original control-flow, we move forward with melding.

To compute the melding profitability of a region, first we need to define what conditions needs to be satisfied for two SESE subgraphs to be meldable.

**Definition 6. Meldable SESE subgraphs:** SESE subgraphs  $S_1$  and  $S_2$  where  $S_1$  belongs to the true path and  $S_2$  belongs to the false path are meldable if any one of the following conditions are satisfied,

- 1) Both  $S_1$  and  $S_2$  have more than one basic block and they are structurally similar i.e. isomorphic.
- 2)  $S_1$  is a simple region and  $S_2$  consists of a single basic block or vice versa.
- 3) Both  $S_1$  and  $S_2$  consists of single basic block.

Definition 6 ensures that any two SESE subgraphs that meets any one of these conditions can be melded without introducing additional divergence to the control-flow.

Figure 2 shows three cases where each of these conditions are applicable. In case ①, two SESE subgraphs  $L$  and  $M$  are isomorphic, therefore they can be melded to have the same control-flow structure (CFG  $N$  in Figure 2). Assume that CFG  $L$  and CFG  $M$  are inside a divergent region  $(E, X)$  and there exists no path from  $E$  to  $X$  that goes through both  $L$  and  $M$  (i.e. any thread in warp that executes  $E$  must either go through  $L$  or  $M$  but not both). In the melded CFG  $N$ , basic blocks  $\%C_P$  and  $\%D_Q$  are guaranteed to post-dominate  $E$  and threads can reconverge at these points resulting in reduction in control-flow divergence. Also the structural similarity in case ① ensures that we do not introduce any additional branches into the melded subgraph. melding of

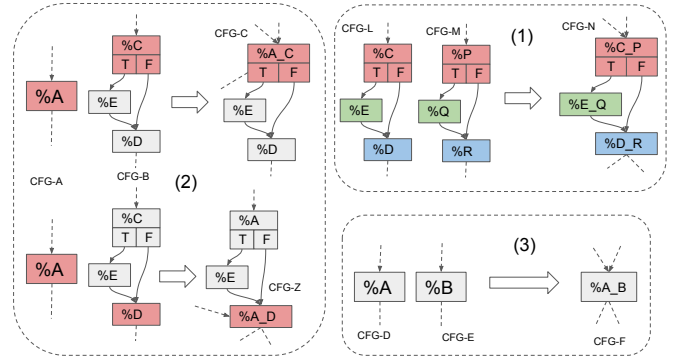


Fig. 2: Example showing the 3 cases considered by CFM to detect meldable subgraphs

non-isomorphic subgraphs is also possible by transforming one subgraph to match the structure of the other, but this is usually expensive and we do not consider this case in our work.

In case ② the melding can be done in two ways, basic block  $\%A$  can be melded with either  $\%C$  or  $\%D$  in CFG  $B$ . Both melded versions (i.e. CFG  $C$  or  $Z$ ) will have less divergence than the original version because threads can reconverge at  $\%A_C$  or  $\%A_D$  respectively. Case ③ is the simplest form where two SESE basic blocks are melded.

A meldable divergent region can potentially have multiple SESE subgraphs in its true and false paths. Therefore we need a strategy to figure out which subgraph pairs to meld. We formulate this as a sequence alignment problem as follows. First, we obtain an ordered sequence of subgraphs in true path and false of the divergent region. Subgraphs are ordered using the post-dominance relation of their entry and exit blocks. For example, if entry node of subgraph  $S_2$  post-dominates exit node of subgraph  $S_1$ , then  $S_2$  comes after  $S_1$  in the order and denoted as  $S_1 \prec S_2$ . A subgraph alignment is defined as follows,

**Definition 7. Subgraph Alignment:** Assume a divergent region  $(E, X)$  has ordered SESE subgraphs  $\{S_1^T, S_2^T, \dots, S_m^T\}$  in its true path and ordered subgraphs  $\{S_1^F, S_2^F, \dots, S_n^F\}$  in the false path. A subgraph alignment is an ordered sequence of tuples  $A = \{(S_{i_0}^T, S_{j_0}^F), (S_{i_1}^T, S_{j_1}^F), \dots, (S_{i_k}^T, S_{j_k}^F)\}$  where,

- 1) if  $(S_p^T, S_q^F) \in A$  then  $S_p^T$  and  $S_q^F$  are meldable subgraphs
- 2) if  $(S_{p_1}^T, S_{q_1}^F) \prec (S_{p_2}^T, S_{q_2}^F)$  then  $S_{p_1}^T \prec S_{p_2}^T$  and  $S_{q_1}^F \prec S_{q_2}^F$

According to definition 7, only meldable subgraphs are allowed in an alignment tuple and if the aligned subgraphs are melded, the resultant control-flow graph does not break the original dominance and post-dominance relations of the subgraphs.

Given a suitable alignment scoring function  $F$  and gap penalty function  $W$ , we can find an optimal subgraph alignment using a sequence alignment method such as Smith-Waterman [18] or Needleman-Wunsch [19] algorithm. The scoring function  $F$  measures the profitability of melding two isomorphic subgraphs  $S_1$  and  $S_2$ . We employ a heuristic to measure this profitability based on instruction frequency in  $S_1$

and  $S_2$ . First we define the melding profitability of two basic blocks  $b_1$  and  $b_2$  as follows,

$$FP_B(b_1, b_2) = \frac{\sum_{i \in Q} \min(\text{freq}(i, b_1), \text{freq}(i, b_2)) \times w_i}{\text{lat}(b_1) + \text{lat}(b_2)}$$

Here  $Q$  is set of all possible instruction types available in the instruction set (*i.e.* LLVM-IR opcodes).  $\text{lat}(b)$  is the static latency of basic block which can be calculated by summing the latencies of all instructions in  $b$ .  $w_i$  is the latency of instruction type  $i$ . The idea here is to approximate the percentage of instruction cycles that can be saved by melding the instructions in  $b_1$  and  $b_2$  assuming a best-case scenario (*i.e.* all common instructions in  $b_1$  and  $b_2$  are melded regardless of their order).

For example, two basic blocks with identical opcode frequency profile will have a profitability value 0.5. Because  $S_1$  and  $S_2$  are isomorphic graphs, there is a one-to-one mapping between basic blocks (*i.e.* corresponding basic blocks). For example, in Figure 2 the the basic block mapping for CFGs  $L$  and  $M$  are  $\{(\%C, \%P), (\%E, \%Q), (\%D, \%R)\}$ .

Assume the mapping of basic blocks in  $S_1$  and  $S_2$  is denoted by  $O$ . Now melding profitability  $FP_S$  of subgraphs  $S_1$  and  $S_2$  can be defined in terms of  $FP_B$  and  $O$ ,

$$FP_S(S_1, S_2) = \frac{\sum_{(b_1, b_2) \in O} FP_B(b_1, b_2) \times (\text{lat}(b_1) + \text{lat}(b_2))}{\sum_{(b_1, b_2) \in O} \text{lat}(b_1) + \text{lat}(b_2)}$$

Similar to  $FP_B$ ,  $FP_S$  measures the percentage of instruction cycles saved by melding two SESE subgraphs. This metric is an over-approximation, however it provides a fast way of measure the melding profitability of two subgraphs that works well in practice. Event though subgraph alignment approach can find the best alignment, we found that using a greedy-approach also works for divergent regions found in real programs because most divergent regions contain small number of subgraphs. In the greedy approach we do  $m \times n$  comparison of subgraphs in true and false path and find the most profitable subgraph pair to meld. In case of a tie we chose a subgraph pair that dominates most of the remaining subgraphs in true and false paths. This ties breaking strategy allows us to perform maximal number of subgraph meldings. We chose to implement this greedy-approach in our implementation of CFM.

**Instruction Alignment:** Notice that our subgraph melding profitability metric (*i.e.*  $FP_S$ ) priorities subgraph pairs that have many similar instructions in their corresponding basic blocks. Therefore when melding two corresponding basic blocks we must ensure that maximum number of similar instructions are melded together. Hence we need to compute an alignment of two instruction sequences such that if they are melded using this alignment, the number of instruction cycles saved will be maximal. A valid instruction alignment is defined similar to definition 7 which ensures that instruction ordering must be preserved in the alignment. For the scoring function, we use *instruction melding profitability* ( $FP_I$ ) which describes

how many instruction cycles can be saved by melding any two instructions  $I_1$  and  $I_2$ .

$$FP_I(I_1, I_2) = \begin{cases} 0 & \text{if } \text{match}(I_1, I_2) \text{ is false} \\ \text{lat}(I_1) - N_s \times l_{sel} & \text{if } \text{match}(I_1, I_2) \text{ is true} \end{cases}$$

Ability to meld for  $I_1$  and  $I_2$  depends on a number of conditions. Some of the important conditions considered here are  $I_1$  and  $I_2$  having the same opcode, having same number of operands, and types of the operands being compatible.  $\text{match}$  is a boolean function that determines the ability to meld of two instructions, and we used the criteria described by Rocha et al. [20] to determine the ability to meld. If two instructions are *not* meldable, the melding profitability is 0, because in that case both instructions need to be executed. If they are meldable only one needs to be executed, so we can save up to  $\text{lat}(I_1)$  cycles. However we need to add *select* instructions to set the correct operands for the melded instruction. Therefore the net profitability is the difference between  $\text{lat}(I_1)$  and the latency of all the selects ( $N_s \times l_{sel}$  term).

Unlike in subgraph alignment, the gap penalty is important for the instruction alignment problem because when there are gaps in the alignment, branches are required to execute the instructions aligned with a gap. However for each gap we only need two branch instructions, one to jump to the unaligned portion and then another to jump back to next aligned section. So the gap penalty is independent of the length of the gap and we use the latency of two branch instructions as the gap penalty. Using the scoring and gap penalty functions described above we apply Needleman-Wunsch algorithm to find an optimal instruction alignment for corresponding basic blocks in two meldable subgraphs.

**Example :** Figure 3a shows the instruction alignment computed for two basic blocks  $A$  and  $B$ . Aligned instructions are shown in green and instructions aligned with a gap are in red.

#### D. CFM Code Generation

CFM’s control-flow melding procedure is shown in algorithm 1. This algorithm takes in a SPMD function  $F$  and iterates over all basic blocks in  $F$  to check if the basic block is an entry to a meldable divergent region ( $R$ ) according to the conditions in Definition 5. We use *Simplify* to convert all subregions inside  $R$  in to simple regions.

The next step is to find the most profitable subgraph pair  $(S_T, S_F)$  that can be melded in the region (*i.e.* *MostProfitableSubgraphPair*). First we compute the optimal subgraph alignment for the two sequences of subgraphs in the true and false paths of  $R$ , and take the most profitable subgraph pair as  $(S_T, S_F)$ . If the melding profitability of this pair is greater than some threshold, we meld the pair. Subgraph melding changes the control-flow of  $F$ , therefore we recompute the control-flow analyses (*e.g.* dominator, post-dominator and region tree) required for the melding pass, and apply it again to  $F$  until no profitable melds can be performed.

Algorithm 2 shows the subgraph melding procedure. The input to this procedure is two isomorphic subgraphs,  $S_T$

---

**Algorithm 1: CFM Algorithm**

---

**Input:** SPMD function  $F$   
**Output:** Melded SPMD function  $F_{out}$

```
do
  changed  $\leftarrow$  false
  for  $BB$  in  $F$  do
     $R, C \leftarrow$  GetRegionFor( $BB$ )
    if  $IsMeldableDivergent(R)$  then
      Simplify( $R$ )
       $(S_T, S_F, profit) \leftarrow$ 
        MostProfitableSubgraphPair( $R$ )
      if  $profit \geq threshold$  then
        Meld( $S_T, S_F, C$ )
        changed  $\leftarrow$  true
        break
      end
    end
  end
end
if changed then
  RecomputeControlFlowAnalyses( $F$ )
end
while changed;
```

---

---

**Algorithm 2: SESE Subgraph melding Algorithm**

---

**Input:** SESE subgraphs  $S_T, S_F$ , Condition  $C$   
**Output:** Melded SESE subgraph  $S_{out}$

```
List blockPairs  $\leftarrow$  Linearize( $S_T, S_F$ )
List A  $\leftarrow$  empty
for  $(B_T, B_F)$  in  $blockPairs$  do
  List instrPairs  $\leftarrow$  ComputeInstrAlignment( $B_T, B_F$ )
  A.append(instrPairs)
end
PreProcess( $S_T, S_F$ )
Map operandMap  $\leftarrow$  empty
for  $P$  in A do
   $I_{melded} \leftarrow$  Clone( $P$ )
  Update(operandMap,  $I_{melded}, P$ )
end
for  $P$  in A do
  SetOperands( $P, operandMap, C$ )
end
RunUnpredication()
RunPostOptimizations()
```

---

and  $S_F$ , and the branching condition  $C$  of the divergent region containing  $S_T$  and  $S_F$ . First the two subgraphs are linearized in pre-order to form a list of corresponding basic block pairs. Processing the basic blocks in pre-order ensures that dominating definitions are melded before their uses. For each basic block pair in this list we compute an optimal alignment of instructions using Needleman-Wunsch to form an instruction alignment for the two subgraphs. Each pair in the alignment falls into two categories,  $I-I$  and  $I-G$ .  $I-I$  is a proper alignment with two instructions and  $I-G$  is an instruction aligned with a gap. Our alignment makes sure that

in a match the two instructions are always meldable into one instruction (e.g. a *load* is not allowed to align with a *store*). First we traverse the alignment pair list and clone the aligned instructions. For  $I-I$  pairs, we clone a single instruction because they can be melded.

During cloning, we also update the *operandMap*, which maintains a mapping between aligned instructions and melded instructions. It also keeps track of the mapping between original basic blocks and melded basic blocks. We perform a second pass over the instruction alignment to set the operands of cloned instructions (*SetOperands*). Assume we are processing an  $I-I$  pair with instructions  $I_T, I_F$  and cloned instruction is  $I_{melded}$ . For each operand of  $I_{melded}$ , the corresponding operands from  $I_T$  and  $I_F$  are looked up in *operandMap* because an operand might be an already melded instruction. If the resultant two operands from  $I_T$  and  $I_F$  are the same, we just use that value as the operand. If they are different, we generate a LLVM *select* to pick the correct operand conditioned by  $C$ . For an  $I-G$  pair, operands are first looked up in *operandMap* and the result is copied to  $I_{melded}$ .

**Example :** Consider the instruction alignment in figure 3a. Figure 3b shows the generated code for aligned instruction pairs ①, ② and ③. In case ①, two select instructions are needed because both operands maps to different values (%0, %4 and %1, %5). In case ②, the first operand is the same (%2) for both instructions, therefore only one select is needed. In case ③, both first and second operands are different for the two instructions. However the second operands map to same melded instruction %7, so only one select is needed. Note that %cmp is the branching condition for the divergent region, and we use that for selecting the operands.

**Melding Branch Instructions:** Setting operands for branch instructions is slightly different than that for other instructions. Note that  $(S_T, S_F)$  and  $S_{melded}$  have the same control-flow structure. Therefore operands for branches inside  $S_{melded}$  are set using the basic block mapping in *operandMap*. Let  $B_T^E, B_F^E$  be the exit blocks of  $S_T$  and  $S_F$ . Successors  $B_T^E, B_F^E$  can contain  $\phi$  nodes. Therefore we need to ensure that successors of  $B_T^E$  and  $B_F^E$  can distinguish values produced in true path or false path. To solve this problem we create two new basic blocks,  $B_T'$  and  $B_F'$ . Next we move the branch conditions of  $B_T^E$  and  $B_F^E$  in to  $B_T'$  and  $B_F'$ . Now we can conditionally branch to  $B_T'$  and  $B_F'$  depending on  $C$  to ensure the correct successors of  $B_T^E$  and  $B_F^E$  are executed next. For example, in Figure 5c basic blocks %M and %N are created when when melding the exit branches of %X1 and %X2 in figure 5b. Any  $\phi$  node in %G (figure 5c) can distinguish the values produced in true or false path using %M and %N.

**Melding  $\phi$  Nodes :** In LLVM SSA form  $\phi$  nodes are always placed at the beginning of a basic block. Even if the instruction alignment result contains two aligned  $\phi$  nodes we can not meld them into a single  $\phi$  node because *select* instructions can not be inserted before them. Therefore we copy all  $\phi$  nodes into the melded basic block and set the operands for them using the *operandMap*. This can introduce redundant  $\phi$  nodes which we remove as a post-processing step.



### E. Unpredication

In our code generation process, we do not execute unaligned instructions conditionally, meaning that unaligned instructions are inserted to the same melded basic block regardless of whether they are from true or false paths. This can introduce overhead due to several reasons. If the branching conditions  $C$  is biased towards the true or false path, it can result in redundant instruction execution. Even if the branch is unbiased, executing instructions from both true and false paths can result in excessive GPGPU power consumption. *Unpredication* splits the melded basic blocks at gap boundaries and moves the unaligned instructions into new blocks.

Figure 3c shows unpredication applied to the unaligned instructions of basic block  $B$  in Figure 3a. The original basic block is split to two parts ( $\%M$  and  $\%M.tail$ ) and unaligned instructions ( $\%8$  and  $\%9$ ) are moved to a new basic block,  $\%M.split$ . Instructions  $\%8$  and  $\%9$  do not dominate any of their uses, therefore  $\phi$  nodes ( $\%10$  and  $\%11$ ) are added to ensure the value flow.  $\%8$  and  $\%9$  are only executed in the false path, therefore we use LLVM undefined value (*undef*) as the incoming value from basic block  $\%M$  in the  $\phi$  nodes. Note that the undefined value is never used because  $\%8$  and  $\%9$  is never executed in the true path.

### F. Pre and Post Processing Steps

In SSA form, any definition must dominate all its uses. However CFM’s subgraph melding can break this property. Consider the example shown in Figure 4.  $S_T$  and  $S_F$  are two meldable subgraphs (Figure 4 A). Definition  $\%a$  dominates its use  $\%x$  before the melding. However if  $S_T$  and  $S_F$  are melded naively then  $\%a$  will no longer dominate  $\%x$ . To fix this we add a new basic block  $\%P$  with a  $\phi$  node  $\%m$ . All uses of  $\%a$  are replaced with  $\%m$  (Figure 4 B). Notice that value  $\%m$  is never meant to be used in the true path execution. Therefore it is undefined in true path (*undef*). We apply this preprocessing step before the melding (*PreProcess* in Algorithm 2).

Subgraph melding can introduce redundant basic blocks, branches and  $\phi$  nodes. Therefore we perform optimizations after the melding to remove redundancies (*RunPostOptimizations* in Algorithm 2). These optimizations include removing branches with identical successors, removing identical operands from  $\phi$  nodes and removing redundant  $\phi$  nodes. After applying the melding algorithm to the input function, we further optimize it using LLVM’s built-in passes (such as the *SimplifyCFG* pass).

### G. Putting it all together

Figure 5 shows how each stage of the subgraph melding pipeline transforms the CFG of the bitonicSort kernel. The original CFG is shown in Figure 5a. Region ( $\%B$ ,  $\%G$ ) is a meldable divergent region.

Figure 5b shows the CFG after region simplification. Subgraphs ( $\%C$ ,  $\%X1$ ) and ( $\%D$ ,  $\%X2$ ) are profitable to meld according to our analysis. Figure 5c shows the CFG after subgraph melding. The result after applying unpredication is shown in Figure 5d. Notice that unpredication splits the basic

block  $\%C_D$  (in Figure 5c) into 5 basic blocks (shown in blue). Basic blocks  $\%P.S.1$  and  $\%P.S.2$  are the unaligned groups of instructions and they are executed conditionally. Figure 5e shows the final optimized CFG after applying post optimizations. Note that *ROCm HIPCC* compiler applied *if-conversion* aggressively. Therefore the effect of unpredication step is nullified in this case.

## V. IMPLEMENTATION

We implemented the CFM algorithm described in section IV as an LLVM-IR analysis and transformation pass on top of the *ROCm HIPCC*<sup>1</sup> GPU compiler [10]. Both the analysis and transformation passes operate on on GPGPU function at a time (*i.e.* they are function passes). The analysis pass first detects meldable divergent regions using LLVM’s divergence analysis. Then it finds the best subgraph pair to meld based on the melding profitability and computes the instruction alignment for corresponding basic blocks (Section IV-C) in the best subgraph pair. For the instruction alignment computation we used the Needleman-Wunsch [19] algorithm implemented by Rocha et al. [20].

The transformation pass uses the analysis computed by the analysis pass to perform CFM’s code generation procedure (Section IV-D). The transformation pass also performs the unpredication, pre- and post-processing steps described in Sections IV-E and IV-F. The LLVM pass is implemented in  $\sim 2500$  lines of C++ code.

### A. Modifications to Compilation Flow

Our pass operates on LLVM-IR. In order to produce the program binary with our pass, we had to include our pass in the *ROCm HIPCC* compilation pipeline. Most GPGPU compilers (*e.g.* CUDA *nvcc*, *ROCm HIPCC*) uses *separate compilation*. In separate compilation, the GPU device code and CPU host code are compiled separately and GPU binary is embedded in the host binary to produce a final executable. In the modified workflow, we first compile the device code into LLVM-IR and run CFM on top of that to produce a transformed IR module. Our pass runs only on device functions and avoids any modifications to host code. After that we use the LLVM static compiler (*lbc*) [21] to generate an object file for the transformed device code. The rest of the compilation flow is the same as one without the modification.

## VI. EVALUATION

### A. Evaluation Setup and Benchmarks

To evaluate the performance of CFM on a machine with a *AMD Radeon RX Vega 64* GPU. This GPU has 8 GBs of global memory, 64 kB of shared memory (*i.e.* Local Data Share (LDS)) and 1590 MHz of max clock frequency. The machine consists of *AMD Ryzen 5 2400G* CPU with 3600 MHz max clock frequency.

We use two different sets of benchmarks. First, to assess the generality of CFM, we create several synthetic benchmarks

<sup>1</sup>LLVM version 12.0.0

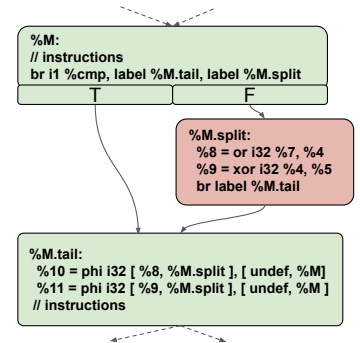
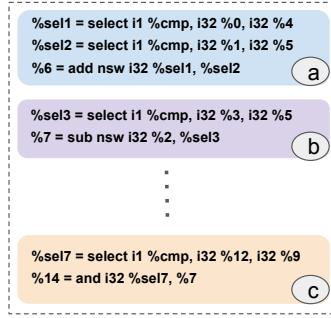
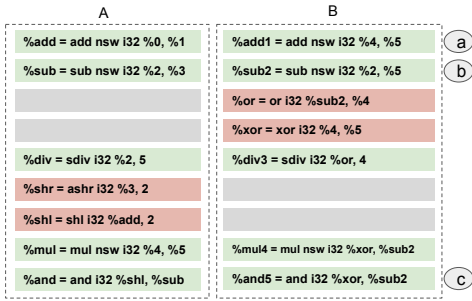


Fig. 3: (a) - Instruction alignment result for two basic blocks *A* and *B*, (b) - Code generated by CFM for aligned instructions ①, ② and ③ in Figure 3a, (c) - Unpredication applied to the unaligned instructions of basic block *B* in figure 3a

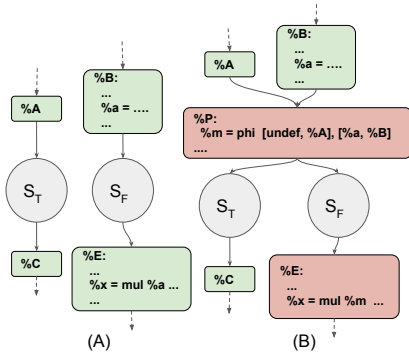


Fig. 4: CFM Pre processing example

that exhibit control divergence of varying complexity. While many real-world programs are hand-optimized to eliminate divergence, these synthetic benchmarks both qualitatively demonstrate the generality of CFM over prior automated divergence-control techniques, and show that CFM can automate the control flow melding that would otherwise have to be done by hand.

**Synthetic Benchmarks** We evaluate six microbenchmarks. SB1, SB2, and SB3, as well as “random” variants of these that we denote SB1-R, SB2-R, and SB3-R.

Each synthetic kernel consists of two nested loops. The inner loop has a divergent *if-then-else* region. Each kernel takes in 4 input variables  $a, b, p$  and  $q$ . The *if* section only operates on  $a, b$  and the *else* section on  $p, q$ . Figure 6 shows the control-flow pattern of this *if-then-else* section for each kernel. SB1 has simple diamond shaped control-flow with basic blocks A2 and A3 performing identical computations. In SB2 and SB3; circled regions are *if-then* sections. *Then* blocks in region pairs B2-B3 (in SB2), C2-C3 and C6-C5 (in SB3) consist of identical computations and therefore melding profitability is high. Kernels SB1-R, SB2-R and SB3-R have identical control-flow structure as SB1, SB2 and SB3 but all the *then* sections perform non-identical computations. All synthetic benchmarks copy the input variables into shared memory and perform the computation and write back again to global memory. We used randomly generated arrays of size  $2^{20}$  for each input variable.

Note neither of the two prior control-flow melding techniques (tail merging [4] and branch fusion [5]) can meld the full set of synthetic benchmarks that we evaluate. Tail merging can partially combine the divergent paths in SB1, SB2, and SB3, but cannot fully merge the divergent regions. It cannot merge the -R variants of any of the synthetic benchmarks due to the different instructions in the divergent paths. Branch fusion subsumes tail merging, and can further fully merge SB1 and SB1-R. However, it cannot be applied to the more complex control flow of SB2 and SB3, or their -R variants.

**Real-world Benchmarks** Second, to show CFM’s effectiveness on real-world divergent benchmarks, we consider 5 real-world programs written in *HIP* [7].

**LUD** An LU-Decomposition kernel from the Rodinia benchmark suite [22]. We focus our evaluation on the *lud\_perimeter* kernel in this benchmark. *lud\_perimeter* contains multiple divergent branches, and branching condition depends on thread ID and block size. We use a randomly generated matrix of size  $16384 \times 16384$  as the input. Branch fusion can successfully merge divergent control-flow in LUD when the loop is unrolled.

**Bitonic Sort** Our running example is bitonic sort [14]. In this kernel, each thread block takes in an input array and performs a parallel bitonic sort. Multiple buckets of numbers are sorted in multiple thread blocks. We used a fixed input size of  $2^{26}$  elements and varied the bucket size (*i.e.* block size). Branch fusion cannot handle the control-flow in Bitonic Sort.

**DCT Quantization** An in-place quantization of a given discrete cosine transformation (DCT) plane using a quantization matrix [23]. The quantization process is different for positive and negative values resulting in data-dependent control-flow divergence. We use a randomly generated DCT plane with size  $2^{15} \times 2^{15}$  as our input. Branch fusion can handle the control flow of DCT.

**Merge sort** A parallel bottom-up mergesort implementation. The kernel has data-dependent control-flow divergence in the merging step. We used an input array with  $2^{20}$  elements. Merge sort has simple diamond control flow, so can be handled by Branch fusion.



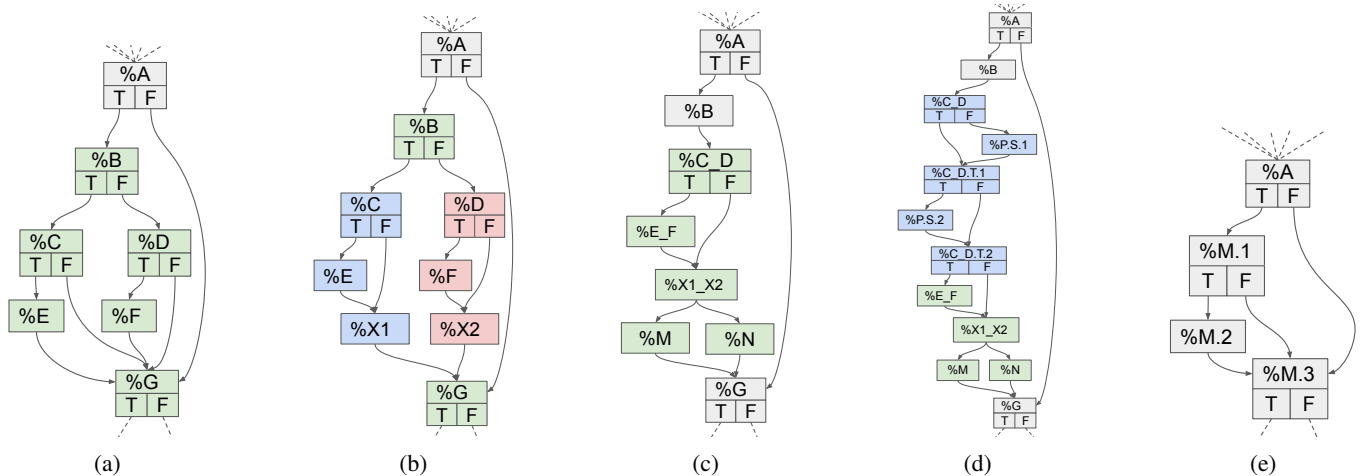


Fig. 5: CFM melding algorithm applied to bitonic sort (Figure 1) (a) - Original control-flow graph, (b) - Region simplification, (c) - CFM subgraph melding, (d) - Unpredication, (e) - Final optimized control-flow graph

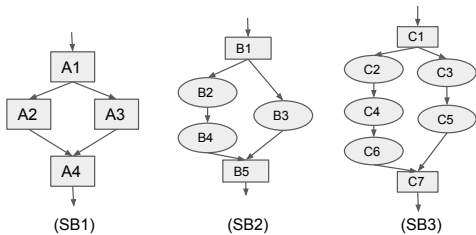


Fig. 6: Control-flow patterns in synthetic benchmarks. Squares are basic blocks and circles are *if-then* regions

**Partition and Concurrent Merge (PCM)** PCM is a parallel sorting algorithm based on Batcher’s odd-even mergesort [24]. PCM performs odd-even merging of *buckets* of sorted elements at every position of the array leading to loops with nested data dependent branches. In our experiments, we used an array of  $2^{28}$  elements with different number of buckets. PCM’s control flow is too complex for Branch fusion to merge.

**Baseline:** Our baseline implementations of these kernels have been hand-optimized (except, obviously, for optimizations that manually remove control divergence by applying CFM-like transformations). This optimization includes using shared memory when needed to improve performance. The baseline implementations were compiled with `-O3`.

**Block size:** Each of these kernels has a tunable *block size*—essentially, a tile size that controls the granularity of work in the inner loops. Because the correct block size can be dependent on many parameters (though for a given input and GPU configuration, one is likely the best), our evaluation treats block size as exogenous to the evaluation, and hence considers behavior at different block sizes for each kernel. In other words, our evaluation asks: if a programmer has a kernel with a given block size, what will happen if CFM is applied?

Note that of these kernels, all but LUD exhibit *odd-even* divergence or data-dependant divergence causing the threads to take different paths through the program. This means that regardless of the block size, the benchmarks will experience

divergence. LUD’s divergence, on the other hand, is block size dependent. For some block sizes, the kernel will be divergent, while for others, it will be convergent.

### B. Performance

Figure 7 shows the speedups for the synthetic benchmarks with different block sizes. CFM can successfully meld all 3 control-flow patterns we consider and gives a superior performance than the baseline for all variants (1.32x geo-mean speedup). The performance for `-R` variants are slightly lower for each of the patterns. This is because `-R` variants contain random instruction sequences and instructions do not align perfectly, causing CFM to insert *select* instructions and branches to unpredicate unaligned instruction groups. We observed higher performance improvement for SB3 and SB3-R compared to the rest because CFM melds multiple subgraph pairs in the SB3 control-flow pattern (Figure 6) and control-flow divergence is reduced more in this case.

Figure 8 shows the speedups for real benchmarks (error bars are not shown as they are negligible, and too small to be visible). CFM always improves the performance ( $1.15\times$  geo-mean speedup over all benchmark  $\times$  block size variants) except for DCT-8X8 where we observed a statistically insignificant 0.21% slow down.

The highest relative improvement in performance can be seen in bitonic sort and PCM benchmarks for all block sizes. This is because both these benchmarks are divergent regardless of the block size and they have complex control-flow regions with shared memory instructions. CFM is able to successfully meld these regions and reduce divergence significantly. The presence of shared memory operations in the divergent regions is key to the performance improvement, as we discuss further in Section VI-D. In LUD, the divergence is block size dependent, and the kernel is divergent only at block sizes 16, 32 and 64 where we see a visible performance improvement introduced by CFM.

For each benchmark, the block size that gives the best performance *for the baseline* is highlighted using a ‘+’ symbol.

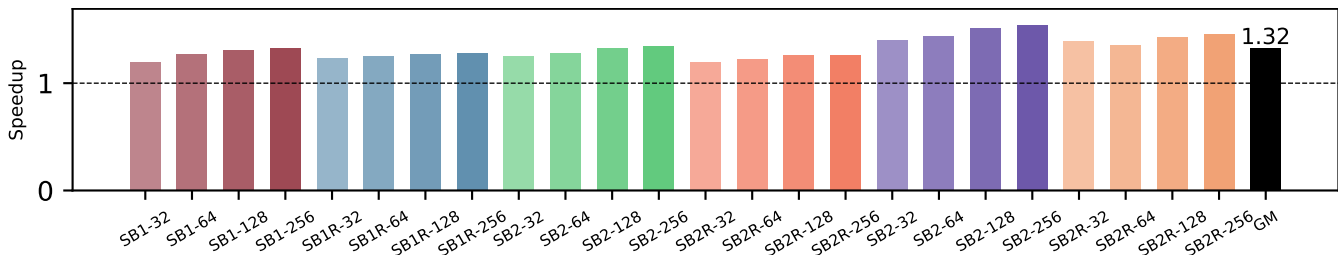


Fig. 7: Micro Benchmark Performance. GM is geomean of CFM’s speedup over baseline.

In all these cases, this is also the block size that gives the best absolute performance for CFM. Interestingly, for 2/5 benchmarks (BIT and MS), not only does this best baseline block size produce the best absolute CFM performance, it also produces the best *speedup* relative to the baseline: the block size that makes the baseline perform the best actually exposes more optimization opportunities to CFM. We believe this is again due to the impact of shared memory operations, as discussed in Section VI-D. Note that LUD’s best performing configuration is one that does not suffer divergence, and in that scenario, CFM does not cause any slowdowns. Because CFM occasionally delivers its best speedup for the best-performing baseline block size, and never results in a slowdown, the geometric mean of the *best blocksize* speedups (GM-Best in Figure 8) is slightly higher than the geometric mean across all benchmarks.

To understand why CFM improves performance we investigate its effects on ALU utilization and memory instructions issued. We used *rocprof* [25] to obtain these hardware metrics. We focus on the block sizes for each benchmark where CFM has highest improvement over the baseline.

### C. ALU Utilization

CFM’s melding transformation enables the ALU instructions in divergent control-paths to be issued in the same cycle. This effectively improves the SIMD resource utilization. Figure 9 shows the ALU utilization (%) for synthetic and real world benchmarks. As expected CFM improves the ALU utilization significantly for all benchmarks except for bitonic sort. In bitonic sort, ALU instructions that appear in divergent paths can not be melded ( $>$  and  $<$  comparisons in lines 9 and 13 in Figure 1). Even though CFM unpredicates these instructions, later optimization passes decide to predicate them again, resulting in both operations being performed in melded control-flow. That and additional *select* instructions added by CFM causes the ALU utilization to go down.

### D. Melding of Memory Instructions

Figure 10 shows the number of memory instructions issued after applying CFM. We report the counts for 3 types of memory instructions that are present in AMD-Vega ISA [26]. These are vector memory, shared memory and flat memory instructions. Vector memory instructions access the global memory and flat memory instructions operate on a flat address space, therefore can access both global and shared memory. All instruction counts are normalized to the baseline counters. In synthetic benchmarks all computations inside the melded

TABLE II: Average Compile Time in seconds

Benchmark	O3	CFM	Normalized
LUD	2.3754	3.7209	1.5664
BIT	0.6690	0.6663	0.9960
DCT	0.6178	0.6207	1.0047
MS	0.9633	0.9699	1.0068
PCM	1.0427	1.2320	1.1816

regions use shared memory. Therefore the number of shared memory instructions issued is far less compared to the baseline for all synthetic benchmarks. Also the reduction in shared memory instructions is higher for SB-1,SB-2 and SB-3 compared to their -R variants because the memory instructions in melded regions align perfectly.

In LUD, the number of shared memory instructions is increased slightly due to predication by later passes. However both vector memory and flat memory instructions have reduced. In bitonic sort and PCM, the melded regions contain a lot of shared memory instructions. Therefore the reduction in shared memory instructions is significant. We find that melding shared memory instructions is more beneficial than melding ALU instructions because shared memory instructions have higher latency than most ALU instructions, though lower latency than global memory instructions. Therefore there is 2X improvement in cycles spent if two divergent shared memory instructions are issued in the same cycle.

### E. Compile Time

Table II shows the compile times for the baseline and CFM. We only report the time to produce device object code and omit the time spent in compiling host code and linking because that is constant for both the baseline and CFM. For three of the five benchmarks, the increased compile time due to CFM is negligible. The exceptions are LUD and PCM, which have a 57% and 18% higher compile time, respectively, which we explain next.

The most time consuming parts of CFM algorithm is the instruction alignment step and greedy subgraph melding profitability computation. The Needleman-Wunsch sequence alignment algorithm we used has a time complexity of  $O(mn)$  where  $m$  and  $n$  are the lengths of the two sequences. LUD has diamond shaped control-flow with *if* and *else* sections of the diamond shape having hundreds of instructions, meaning instruction alignment consumes a substantial amount of time. In the greedy subgraph melding profitability computation, we compare each subgraph in the true path with every subgraph in

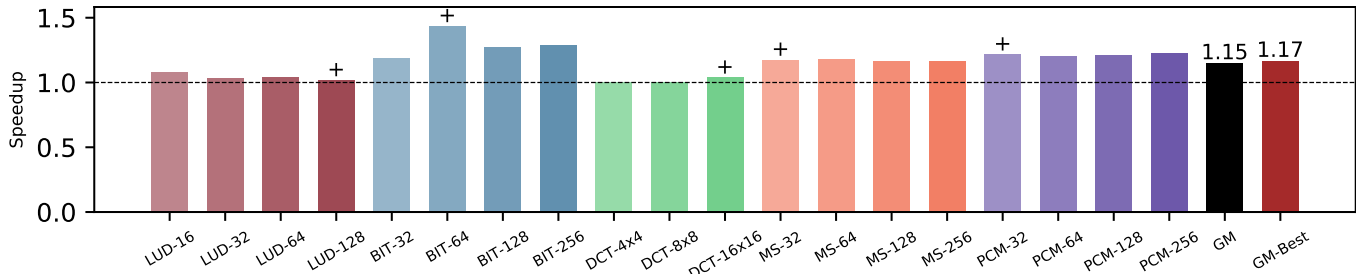


Fig. 8: Real World Benchmark Performance. + marks block size with best baseline runtime. GM is geomean of CFM’s speedup on all benchmarks; GM-best is CFM’s speedup on + configurations.

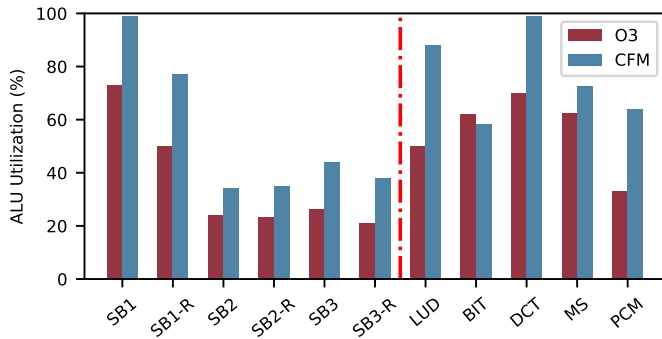


Fig. 9: ALU Utilization

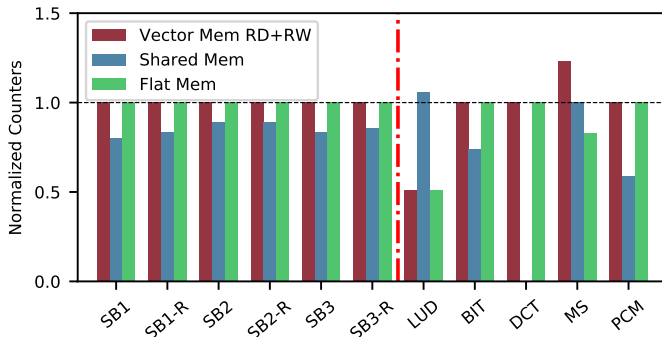


Fig. 10: Normalized Memory Instruction Counters

the false path. This comparison is expensive if there are many subgraphs in the divergent region. In PCM, both sides of the divergent branch contains loops. These loops gets unrolled and form multiple isomorphic regions in the true and false paths. Even though the basic blocks in these regions are small, CFM still needs to performs an  $N \times M$  similarity comparison to find a profitable subgraph pair to meld, resulting in increased compilation time.

## VII. RELATED WORK

*a) Divergence Analysis:* Reducing control flow divergence requires finding the source of divergence in a program. Coutinho *et al.* constructed a divergence analysis to statically identify variables with the same value for every SIMD unit and used this analysis to drive branch fusion [5]. A divergence analysis of similar fashion based on data dependences and sync dependences has been integrated to the LLVM framework [12]. More recently, Rosemann *et al.* has presented a general and precise divergence analysis based on abstract interpretation for reducible CFGs [13].

*b) Code Compaction: Tail Merging or Cross Jumping* is a standard, but restrictive, compiler optimization used to reduce the size of the code by merging identical sequences of instructions. Chen *et al.* used a generalized version of tail merging to compact matching *Single-Entry-Multiple-Exit* regions [4]. Recently, Rocha *et al.* has presented *Function Merging*, an advanced sequence-alignment based technique for code size reduction [20], [27]. Even though parts of CFM has some similarities with function merging, especially the sequence alignment part, function merging does not tackle divergence.

*c) Compiler Techniques:* Several techniques have been proposed to reduce divergence through compiler transformations. Coutinho *et al.* introduced fusing branches with a strong divergence analysis [5]. But their technique is applicable only for CFGs with a diamond pattern. Anantpur and Govindarajan proposed an algorithm to transform unstructured CFGs to structured ones and then properly linearize it with predication [28]. More recently, Fukuhara and Takimoto proposed *Speculative Sparse Code Motion* to reduce branch divergence in GPU programs [29]. This technique does not alter the structure of the CFG and is orthogonal to CFM.

Another the compiler optimization for reducing control flow divergence is *Iteration Delaying* which delays loop iterations that take a different branch [30]. Iteration delaying is complementary to CFM and can be applied after performing our optimization. Recently Damani *et al.* has presented a speculative reconvergence technique for GPUs similar to iteration delaying [31]. *Collaborative Context Collection* is technique that, when faced with thread-divergent warps in GPUs, makes copies of relevant registers to shared memory and only restores them when the warps become non-divergent [32].

*d) Hardware Techniques:* Many hardware techniques have been proposed to reduce thread divergence. Thread Block Compaction [33] and Dynamic Warp Formation [1] involve repacking threads into non-divergent warps. Variable Warp Sizing [34] and Dynamic Warp Subdivision [35] depend on smaller warps to schedule divergent thread groups in parallel. Independent Thread Scheduling helps to hide the latency in divergent paths by allowing to switch between divergent threads inside a warp [3], [36].

## VIII. CONCLUSION

Divergent control-flow in GPGPU programs can cause significant performance degradation because thread execution

needs to be serialized if threads in a warp exercise different control-flow paths. We presented CFM, a new compiler analysis and transformation framework for GPGPU programs that can detect similar control-flow regions in divergent paths and meld them to produce a new control-flow graph with fewer divergent instructions. CFM generalizes and subsumes prior efforts at reducing divergence such as tail merging and branch fusion, melding control flow for complex CFGs while avoiding performance degradation even for code that is dynamically non-divergent. We implemented CFM on LLVM and showed that CFM improves performance by improving ALU utilization and promoting coalesced memory accesses across several real-world benchmarks.

## REFERENCES

- [1] W. W. L. Fung, I. Sham, G. Yuan, and T. M. Aamodt, "Dynamic warp formation and scheduling for efficient gpu control flow," in *40th Annual IEEE/ACM International Symposium on Microarchitecture (MICRO 2007)*, 2007, pp. 407–420.
- [2] W. W. L. Fung and T. M. Aamodt, "Thread block compaction for efficient simt control flow," in *2011 IEEE 17th International Symposium on High Performance Computer Architecture*, 2011, pp. 25–36.
- [3] M. Rhu and M. Erez, "The dual-path execution model for efficient gpu control flow," in *2013 IEEE 19th International Symposium on High Performance Computer Architecture (HPCA)*, 2013, pp. 591–602.
- [4] W.-K. Chen, B. Li, and R. Gupta, "Code compaction of matching single-entry multiple-exit regions," in *Proceedings of the 10th International Conference on Static Analysis*, ser. SAS'03. Berlin, Heidelberg: Springer-Verlag, 2003, p. 401–417.
- [5] B. Coutinho, D. Sampaio, F. M. Q. Pereira, and W. Meira Jr., "Divergence analysis and optimizations," in *2011 International Conference on Parallel Architectures and Compilation Techniques*, 2011, pp. 320–329.
- [6] C. Lattner and V. Adve, "Llvm: a compilation framework for lifelong program analysis transformation," in *International Symposium on Code Generation and Optimization, 2004. CGO 2004.*, 2004, pp. 75–86.
- [7] "HIP Programming Guide v4.1," <https://rocmdocs.amd.com/en/latest/>, [Online; accessed 17-April-2021].
- [8] "CUDA C++ Programming Guide," <https://docs.nvidia.com/cuda/cuda-c-programming-guide/index.html>, [Online; accessed 17-April-2021].
- [9] "NVCC :: CUDA Toolkit Documentation," <https://docs.nvidia.com/cuda/cuda-compiler-driver-nvcc/index.html>, [Online; accessed 17-April-2021].
- [10] "ROCm Compiler SDK," [https://rocmdocs.amd.com/en/latest/ROCm\\_Compiler\\_SDK/ROCm-Compiler-SDK.html](https://rocmdocs.amd.com/en/latest/ROCm_Compiler_SDK/ROCm-Compiler-SDK.html), [Online; accessed 17-April-2021].
- [11] R. Cytron, J. Ferrante, B. K. Rosen, M. N. Wegman, and F. K. Zadeck, "Efficiently computing static single assignment form and the control dependence graph," *ACM Trans. Program. Lang. Syst.*, vol. 13, no. 4, p. 451–490, Oct. 1991. [Online]. Available: <https://doi.org/10.1145/115372.115320>
- [12] R. Karrenberg and S. Hack, "Improving performance of opencl on cpus," in *Compiler Construction*, M. O'Boyle, Ed. Berlin, Heidelberg: Springer Berlin Heidelberg, 2012, pp. 1–20.
- [13] J. Rosemann, S. Moll, and S. Hack, "An abstract interpretation for spmd divergence on reducible control flow graphs," *Proc. ACM Program. Lang.*, vol. 5, no. POPL, Jan. 2021. [Online]. Available: <https://doi.org/10.1145/3434312>
- [14] K. E. Batcher, "Sorting networks and their applications," in *Proceedings of the April 30–May 2, 1968, spring joint computer conference (AFIPS '68 (Spring))*, 1968, p. 307–314.
- [15] D. Cederman and P. Tsigas, "Gpu-quicksort: A practical quicksort algorithm for graphics processors," *ACM J. Exp. Algorithmics*, vol. 14, Jan. 2010. [Online]. Available: <https://doi.org/10.1145/1498698.1564500>
- [16] "llvm::RegionBase Class Template Reference," [https://llvm.org/doxygen/classllvm\\_1\\_1RegionBase.html](https://llvm.org/doxygen/classllvm_1_1RegionBase.html), [Online; accessed 17-April-2021].
- [17] R. Johnson, D. Pearson, and K. Pingali, "The program structure tree: Computing control regions in linear time," *SIGPLAN Not.*, vol. 29, no. 6, p. 171–185, Jun. 1994. [Online]. Available: <https://doi.org/10.1145/773473.178258>
- [18] T. Smith and M. Waterman, "Identification of common molecular subsequences," *Journal of Molecular Biology*, vol. 147, no. 1, pp. 195–197, 1981. [Online]. Available: <https://www.sciencedirect.com/science/article/pii/0022283681900875>
- [19] S. B. Needleman and C. D. Wunsch, "A general method applicable to the search for similarities in the amino acid sequence of two proteins," *Journal of Molecular Biology*, vol. 48, no. 3, pp. 443–453, 1970. [Online]. Available: <https://www.sciencedirect.com/science/article/pii/0022283670900574>
- [20] R. C. O. Rocha, P. Petoumenos, Z. Wang, M. Cole, and H. Leather, "Effective function merging in the ssa form," in *Proceedings of the 41st ACM SIGPLAN Conference on Programming Language Design and Implementation*, ser. PLDI 2020. New York, NY, USA: Association for Computing Machinery, 2020, p. 854–868. [Online]. Available: <https://doi.org/10.1145/3385412.3386030>
- [21] "llc - LLVM static compiler," <https://llvm.org/docs/CommandGuide/llc.html>, [Online; accessed 17-April-2021].
- [22] S. Che, M. Boyer, J. Meng, D. Tarjan, J. W. Sheaffer, S. Lee, and K. Skadron, "Rodinia: A benchmark suite for heterogeneous computing," in *2009 IEEE International Symposium on Workload Characterization (IISWC)*, 2009, pp. 44–54.
- [23] "CUDA Samples," <https://docs.nvidia.com/cuda/cuda-samples/>, [Online; accessed 17-April-2021].
- [24] E. Herruzo, G. Ruiz, J. I. Benavides, and O. Plata, "A new parallel sorting algorithm based on odd-even mergesort," in *15th EUROMICRO International Conference on Parallel, Distributed and Network-Based Processing (PDP'07)*, 2007, pp. 18–22.
- [25] "ROCm-Developer-Tools / rocprofiler," <https://github.com/ROCm-Developer-Tools/rocprofiler>, [Online; accessed 17-April-2021].
- [26] "'Vega' Instruction Set Architecture," [https://rocmdocs.amd.com/en/latest/GCN\\_ISA\\_Manuals/testdocbook.html](https://rocmdocs.amd.com/en/latest/GCN_ISA_Manuals/testdocbook.html), [Online; accessed 17-April-2021].
- [27] R. C. O. Rocha, P. Petoumenos, Z. Wang, M. Cole, and H. Leather, "Function merging by sequence alignment," in *2019 IEEE/ACM International Symposium on Code Generation and Optimization (CGO)*, 2019, pp. 149–163.
- [28] J. Anantpur and G. R., "Taming control divergence in gpus through control flow linearization," in *Compiler Construction*, A. Cohen, Ed. Berlin, Heidelberg: Springer Berlin Heidelberg, 2014, p. 133–153.
- [29] J. Fukuhara and M. Takimoto, "Branch divergence reduction based on code motion," *Journal of Information Processing*, vol. 28, pp. 302–309, 2020.
- [30] T. D. Han and T. S. Abdelrahman, "Reducing branch divergence in gpu programs," in *Proceedings of the Fourth Workshop on General Purpose Processing on Graphics Processing Units*, ser. GPGPU-4. New York, NY, USA: Association for Computing Machinery, 2011. [Online]. Available: <https://doi.org/10.1145/1964179.1964184>
- [31] S. Damani, D. R. Johnson, M. Stephenson, S. W. Keckler, E. Yan, M. McKeown, and O. Giroux, "Speculative reconvergence for improved simt efficiency," in *Proceedings of the 18th ACM/IEEE International Symposium on Code Generation and Optimization*, ser. CGO 2020. New York, NY, USA: Association for Computing Machinery, 2020, p. 121–132. [Online]. Available: <https://doi.org/10.1145/3368826.3377911>
- [32] F. Khorasani, R. Gupta, and L. N. Bhuyan, "Efficient warp execution in presence of divergence with collaborative context collection," in *Proceedings of the 48th International Symposium on Microarchitecture*, ser. MICRO-48. New York, NY, USA: Association for Computing Machinery, 2015, p. 204–215. [Online]. Available: <https://doi.org/10.1145/2830772.2830796>
- [33] W. W. L. Fung and T. M. Aamodt, "Thread block compaction for efficient simt control flow," in *2011 IEEE 17th International Symposium on High Performance Computer Architecture*, 2011, pp. 25–36.
- [34] T. G. Rogers, D. R. Johnson, M. O'Connor, and S. W. Keckler, "A variable warp size architecture," in *Proceedings of the 42nd Annual International Symposium on Computer Architecture*, ser. ISCA '15. New York, NY, USA: Association for Computing Machinery, 2015, p. 489–501. [Online]. Available: <https://doi.org/10.1145/2749469.2750410>
- [35] J. Meng, D. Tarjan, and K. Skadron, "Dynamic warp subdivision for integrated branch and memory divergence tolerance," *SIGARCH*

*Comput. Archit. News*, vol. 38, no. 3, p. 235–246, Jun. 2010. [Online].  
Available: <https://doi.org/10.1145/1816038.1815992>

- [36] A. ElTantawy, J. W. Ma, M. O'Connor, and T. M. Aamodt, "A scalable multi-path microarchitecture for efficient gpu control flow," in *2014 IEEE 20th International Symposium on High Performance Computer Architecture (HPCA)*, 2014, pp. 248–259.